

Novel correlates of protection against pandemic H1N1 influenza A virus infection

Sophia Ng^{1,2,3,9}, Raffael Nachbagauer^{1,3,4,5,9}, Angel Balmaseda^{6,7}, Daniel Stadlbauer^{1,3,4,5}, Sergio Ojeda⁷, Mayuri Patel^{1,2,3}, Arvind Rajabhathor^{1,3,4,5}, Roger Lopez^{6,7}, Andrea F. Guglia⁴, Nery Sanchez⁷, Fatima Amanat^{3,4,5}, Lionel Gresh^{1,7}, Guillermina Kuan^{7,8}, Florian Krammer^{1,3,4,5,10*} and Aubree Gordon^{1,2,3,10*}

Influenza viruses remain a severe threat to human health, causing up to 650,000 deaths annually^{1,2}. Seasonal influenza virus vaccines can prevent infection, but are rendered ineffective by antigenic drift. To provide improved protection from infection, novel influenza virus vaccines that target the conserved epitopes of influenza viruses, specifically those in the hemagglutinin stalk and neuraminidase, are currently being developed³. Antibodies against the hemagglutinin stalk confer protection in animal studies^{4–6}. However, no data exist on natural infections in humans, and these antibodies do not show activity in the hemagglutination inhibition assay, the hemagglutination inhibition titer being the current correlate of protection against influenza virus infection^{7–9}. While previous studies have investigated the protective effect of cellular immune responses and neuraminidase-inhibiting antibodies, additional serological correlates of protection from infection could aid the development of broadly protective or universal influenza virus vaccines^{10–13}. To address this gap, we performed a household transmission study to identify alternative correlates of protection from infection and disease in naturally exposed individuals. Using this study, we determined 50% protective titers and levels for hemagglutination inhibition, full-length hemagglutinin, neuraminidase and hemagglutinin stalk-specific antibodies. Further, we found that hemagglutinin stalk antibodies independently correlated with protection from influenza virus infection.

We followed 300 household members in a Nicaraguan family cohort who lived with 1 of 88 influenza-positive index cases for 3–5 weeks to test for infection and seroconversion (Fig. 1a and Extended Data Fig. 1). The majority of households were recruited during the 2015 season ($n=65$) since pandemic H1N1 influenza virus activity was lower in 2013 ($n=23$). Only ten household members were vaccinated for the concurrent influenza season (Supplementary Table 1), which did not allow for detailed comparisons to unvaccinated individuals. Individuals who reported prior influenza virus vaccination were distributed evenly across antibody levels and two had PCR-confirmed influenza virus infection. Overall, 84 (28%) household members had a PCR-confirmed infection and approximately two-thirds ($n=53$) of PCR-positive individuals developed symptomatic influenza.

To identify the antibody levels associated with protection from infection and disease, we tested baseline (collected on confirmed infection in a household) and follow-up (3–5 weeks post-enrollment) blood samples using the classical hemagglutination inhibition assay as well as enzyme-linked immunosorbent assays (ELISAs) that measured antibodies against full-length hemagglutinin, the hemagglutinin stalk domain or the neuraminidase.

As expected, we found that individuals with higher pre-exposure hemagglutination inhibition titers were less likely to become infected (Fig. 1b). The 50% protective hemagglutination inhibition titer (that is, the antibody level at which the risk of contracting influenza is reduced by 50% compared to individuals without detectable antibodies) was between 1:20 and 1:40, which is consistent with previous studies (Fig. 1b and Supplementary Table 2) (ref. ¹⁴). High baseline ELISA levels measuring full-length hemagglutinin antibodies in individuals who tested negative in the hemagglutinin inhibition assay indicate a strong prevalence of non-hemagglutinin inhibition-active antibodies in the study participants. This can be explained by the presence of antibodies that bind the hemagglutinin protein, but do not sterically interfere with receptor binding, which is the activity measured in the hemagglutination inhibition assay. ELISAs measuring full-length hemagglutinin and neuraminidase antibodies correlated with protection from infection with narrow 95% confidence intervals (CIs). The estimated 50% protective levels for both assays ranged between areas under the curve (AUCs) of 20 and 40 (Fig. 1b and Supplementary Table 2). The CIs were wider for hemagglutinin stalk antibodies, but similar 50% protective levels were between AUCs of 40 and 80.

We additionally estimated crude (that is, not adjusted for age or other variables) 50% protection antibody levels against PCR-confirmed symptomatic influenza and found a similar good correlation with protection for all measured antibody levels. The antibody level associated with 50% protection was approximately 1:40 for the hemagglutination inhibition antibodies and between AUCs of 20 and 40 for full-length hemagglutinin, hemagglutinin stalk and neuraminidase binding antibodies (Fig. 1c, Supplementary Table 3 and Extended Data Figs. 2 and 3).

When preexisting antibody levels of individuals who were either PCR-positive or negative for the influenza virus were plotted side by

¹Department of Epidemiology, School of Public Health, University of Michigan, Ann Arbor, MI, USA. ²St. Jude Center of Excellence for Influenza Research and Surveillance, Memphis, TN, USA. ³Centers of Excellence for Influenza Research and Surveillance, Bethesda, MD, USA. ⁴Department of Microbiology, Icahn School of Medicine at Mount Sinai, New York, NY, USA. ⁵Center for Research on Influenza Pathogenesis, New York, NY, USA. ⁶Laboratorio Nacional de Virología, Centro Nacional de Diagnóstico y Referencia, Ministry of Health, Managua, Nicaragua. ⁷Sustainable Sciences Institute, Managua, Nicaragua. ⁸Centro de Salud Sócrates Flores Vivas, Ministry of Health, Managua, Nicaragua. ⁹These authors contributed equally: S. Ng, R. Nachbagauer.

¹⁰These authors jointly supervised this work: F. Krammer, A. Gordon. *e-mail: florian.krammer@mssm.edu; gordonal@umich.edu

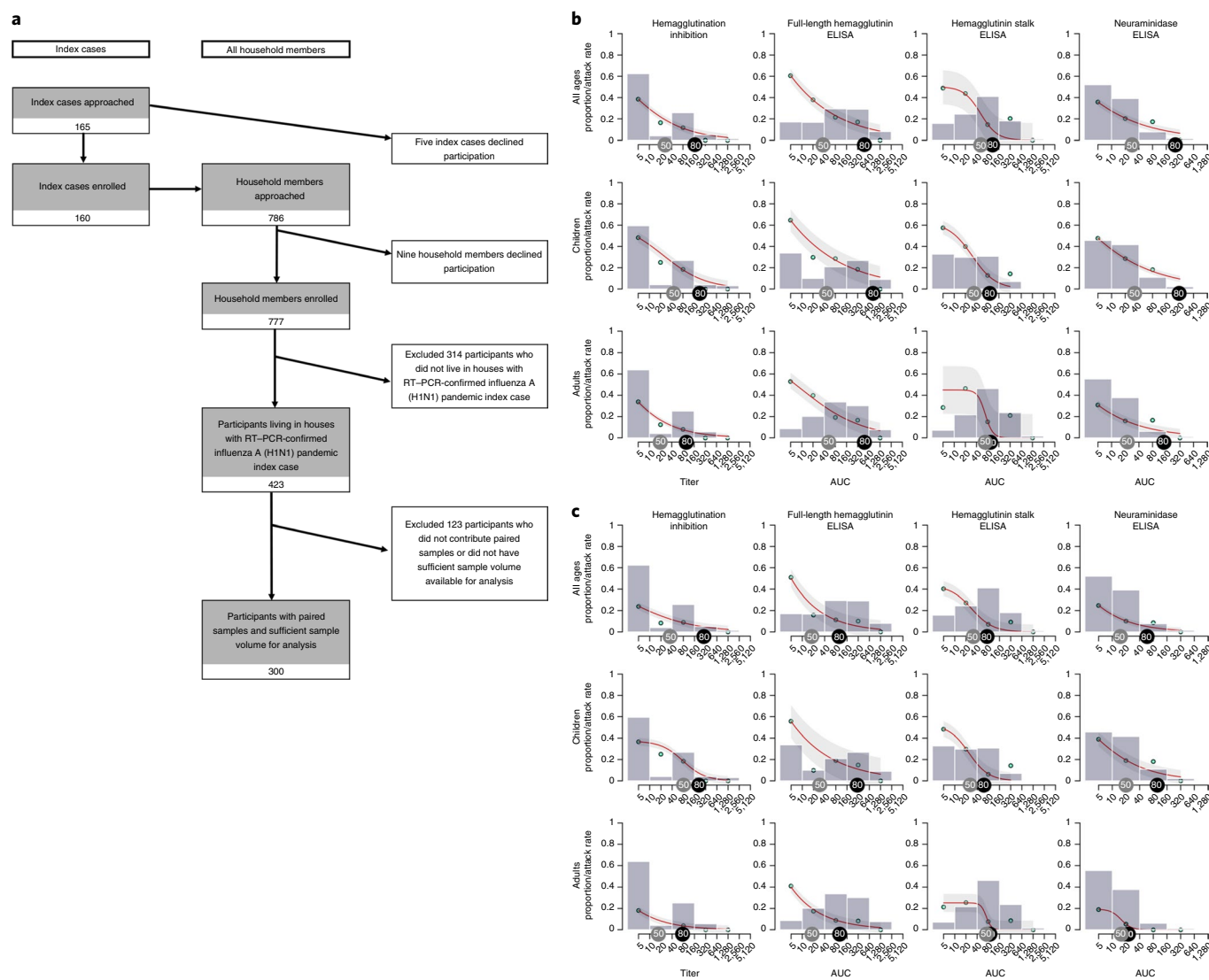


Fig. 1 | Study overview and antibody levels in relation to rates of infection. **a**, Patient enrollment flow chart. **b,c**, The gray bars show the proportion of household contacts having a certain level of preexisting antibody levels. The bars group individuals between the antibody levels covered by the bars on the x axis (for example, the left-most bar includes all individuals with antibody levels <10, followed by 10 but less than 40, etcetera). The red lines fit the antibody-level-specific secondary attack rate (SAR) based on the observed rates, which are indicated as cyan circles. The attack rate was calculated by dividing the number of infected contacts who had a specific baseline antibody level by the total number of contacts who had the same level of antibodies. The light gray shaded areas represent the 95% confidence intervals. The gray tags indicate a 50% protection antibody level, and the black tags indicate an 80% protection antibody level. Analyses were performed combined (all ages, $n = 300$ individuals) as well as separately for children (0–14 years old, $n = 101$ individuals) and adults (15–85 years old, $n = 199$ individuals).

side, a clear trend could be observed (Fig. 2, Extended Data Fig. 4 and Supplementary Tables 4–6). Participants who became infected had very low hemagglutinin and neuraminidase antibody levels. In addition, hemagglutinin stalk antibody levels measured by ELISA were lower in individuals who developed PCR-confirmed symptomatic influenza compared to PCR-confirmed asymptomatic individuals ($P < 0.01$) suggesting that these antibodies correlated with protection from infection and disease.

These crude analyses do not account for the effect of age and other antibodies in protected individuals. Thus, we adjusted for potential correlations by comparing the calculated protective effects associated with a fourfold increase in antibody levels (seroconversion) in a single-assay model, to a multi-assay model that adjusts for correlation with other assays and age.

When adjusted for the effects of other measured antibody levels and age (multi-assay model), we found that hemagglutination

inhibition, full-length hemagglutinin and hemagglutinin stalk antibody levels remained independent predictors of protection against both PCR-confirmed infection and symptomatic influenza (Fig. 3). Antibodies measured against neuraminidase showed a similar trend and were associated with protection against symptomatic influenza when adjusted for hemagglutination inhibition antibodies. However, they were not independently associated with protection when adjusted for both hemagglutination inhibition and hemagglutinin stalk antibodies, indicating that neuraminidase antibodies in these individuals correlated with antibodies that were induced against hemagglutinin. Using the multi-assay model, we found a fourfold increase in hemagglutinin stalk antibodies to be associated with a 42% (CI, 15 and 60%) reduction in risk of being infected, which was slightly lower than the effect observed for a fourfold increase of hemagglutination inhibition antibodies (57%; CI, 35 and 72%). A similar reduction in infection risk was observed for symptomatic

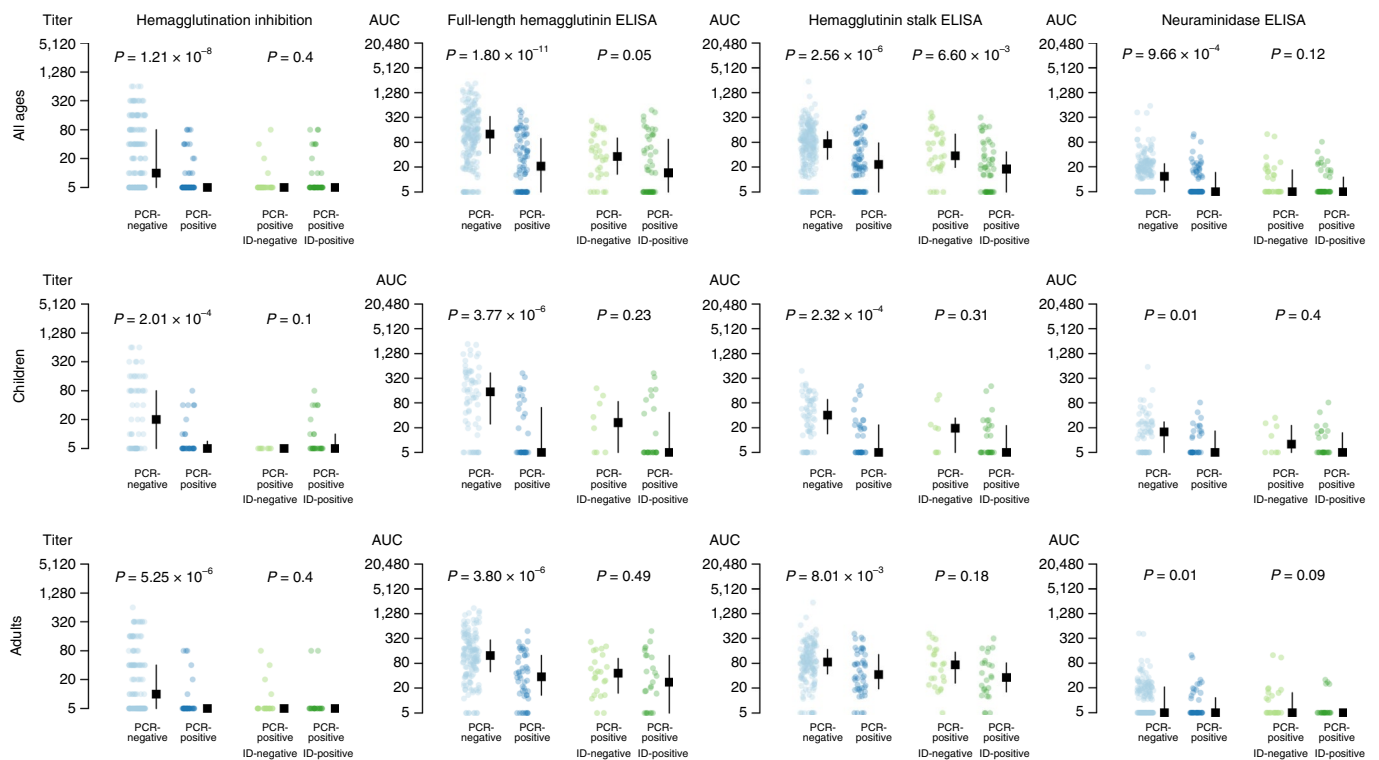


Fig. 2 | Preexisting antibody levels based on influenza outcomes. Antibody levels for each individual, and the median and interquartile range, are shown. The y axis indicates the antibody levels. Individuals were separated by PCR-positivity status (blue dots) and by symptomatic influenza (green dots). Analyses were performed combined (all ages, $n=300$ individuals) as well as separately for children (0–14 years old, $n=101$ individuals) and adults (15–85 years old, $n=199$ individuals). Two-tailed Wilcoxon rank-sum tests were used to calculate the P values. See Supplementary Table 4 for the FDR analyses. Age groups and outcomes were prespecified before analyses. ID, influenza disease.

influenza. Age-stratified results are shown in Extended Data Figs. 5 and 6. These findings provide important support to the notion that non-hemagglutination inhibition active antibodies can be independently predictive of protection from influenza virus infection.

To compare the usefulness of ELISA-based readouts to hemagglutination inhibition for assessing seroconversion, we calculated fold inductions of antibody levels postinfection for PCR-positive and PCR-negative cases (Fig. 4). Consistent with previous studies, we found that 22% of individuals did not respond to infection as measured by hemagglutination inhibition (Fig. 4, light-blue peak at onefold)¹⁵. Interestingly, we did not detect any apparent non-responders using ELISAs measuring full-length hemagglutinin- and hemagglutinin stalk-specific antibodies. Many infected children (64%) did not show an increase in anti-neuraminidase antibody levels. Infection is generally thought to boost neuraminidase antibody levels¹⁶, but measured responses against neuraminidase may be generally low as we found previously¹⁷. A proportion of PCR-negative individuals seroconverted in all assays, which might be attributable to these individuals not shedding enough virus for detection via PCR while still being infected. Additional sensitivity and specificity analyses were performed and indicate that ELISAs are useful to assess seroconversion in addition to hemagglutination inhibition assays (Extended Data Figs. 7 and 8).

Novel universal influenza virus vaccines that elicit broadly reactive antibodies against conserved epitopes in the hemagglutinin stalk domain are currently in clinical development. However, hemagglutinin stalk antibodies have not been shown to correlate with protection against natural influenza virus infection in humans. In this study, we used samples from a household transmission study to examine hemagglutination inhibition, full-length hemagglutinin, hemagglutinin stalk and neuraminidase antibodies as potential

correlates of protection from influenza infection and disease. Importantly, using multiple statistical approaches we showed that hemagglutinin stalk antibodies (which cannot be detected in hemagglutination inhibition assays¹⁰) were associated with protection against pandemic H1N1 influenza virus infection and disease.

Consistent with previous studies, a baseline hemagglutination inhibition titer between 1:20 and 1:40 was predictive of a 50% reduction in PCR-confirmed H1N1 influenza virus infection¹⁴. Interestingly, only few individuals had baseline hemagglutination inhibition titers ranging from 1:10 to 1:40. Instead, titers were either undetectable or higher than 1:40 (Fig. 1). A possible explanation for this could be that the antibodies measured in this largely unvaccinated population were elicited by recent infections because the virus only circulated for 4–6 years before the study; it has been shown that hemagglutination inhibition antibodies elicited by infection are maintained at titers $>1:40$ for many years¹⁸. Using ELISAs that measured antibodies against full-length hemagglutinin, neuraminidase, or specifically the hemagglutinin stalk, we could also identify crude estimates of protection. We found that these results were consistent between two influenza seasons (Extended Data Figs. 2 and 3). Importantly, ELISAs against hemagglutinin can measure antibody levels irrespective of the ability of the virus to agglutinate red blood cells, which is required for hemagglutination inhibition assays and has posed a problem for serology against recent H3N2 virus strains¹⁹. Furthermore, these assays can detect non-neutralizing (but potentially protective) antibodies, which is of importance for anti-stalk antibodies that confer the majority of their protective effect through Fc-mediated functions^{20,21}.

This study demonstrates that levels of hemagglutinin stalk antibodies are a correlate of protection against natural pandemic H1N1 influenza virus infection. While previously published findings from

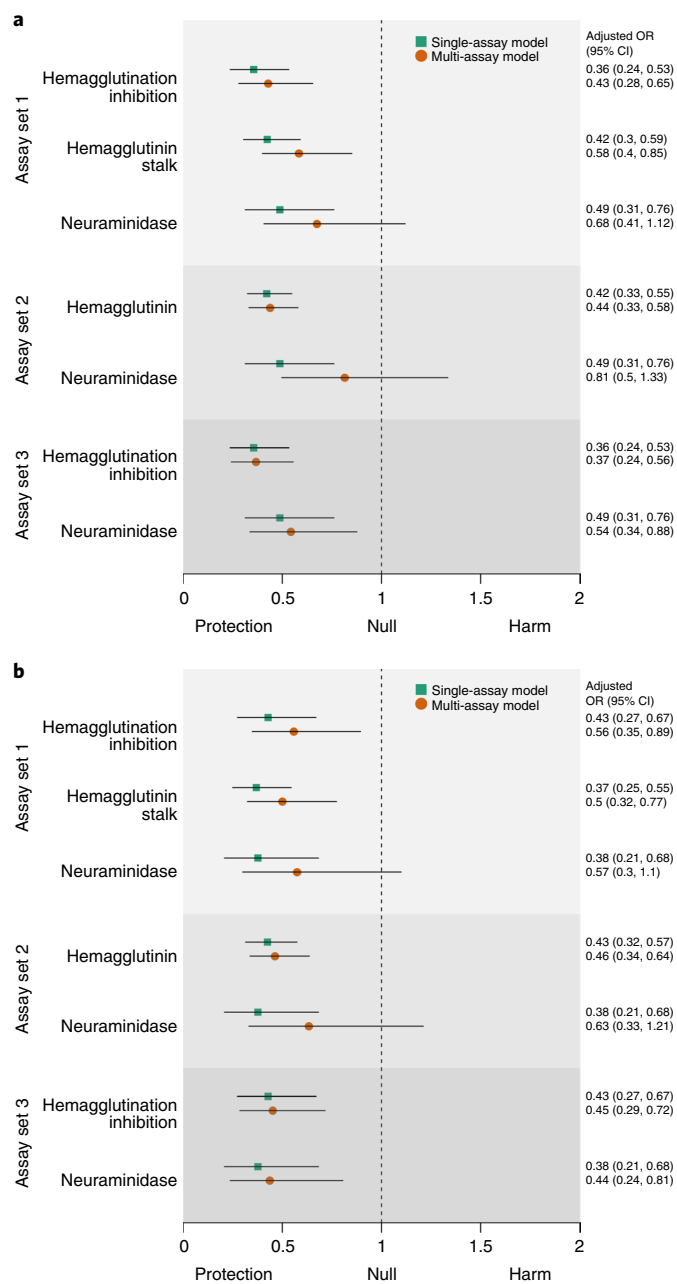


Fig. 3 | Protective effects associated with a fourfold increase in antibody level. Results are shown for three different sets of assays. **a**, PCR-confirmed infection. **b**, Symptomatic influenza ($n=300$ individuals).

Assay set 1 combines hemagglutination inhibition, hemagglutinin stalk and neuraminidase ELISAs. Assay set 2 combines full-length hemagglutinin and neuraminidase ELISAs. Assay set 3 combines hemagglutination inhibition and neuraminidase ELISAs. The adjusted odds ratios (ORs) for the single-assay model are shown as green squares and for the multi-assay model as orange circles. The black lines denote the 95% CIs.

a human challenge model did not find hemagglutinin stalk antibodies to be predictive of protection from infection, they found an association with a reduction in viral shedding²². A possible explanation for this difference is that human volunteers were inoculated intranasally with high doses of infectious particles (approximately 10^7), whereas natural infection is probably caused by much lower particle numbers²³. This difference is further highlighted by the fact that even individuals with high hemagglutination inhibition titers ($>1:1,000$) were not protected from infection in the challenge

setting, which is not consistent with the findings of the majority of vaccine efficacy studies²⁴.

Of note, the CIs in this study for the predicted protective effect of hemagglutinin stalk antibodies for PCR-confirmed infection were wider for adults compared to children (Fig. 1a). Multiple factors may have contributed to this observation. There were few adult individuals who had baseline hemagglutinin stalk antibody levels of <10 , which may have contributed to the lower than expected number of cases. An important observation is the higher than expected number of infections at AUC levels from 160 to 640. This could be an indication that high titers of hemagglutinin stalk antibodies are required for complete virus neutralization, which is consistent with previous observations that hemagglutinin stalk antibodies have lower neutralizing activities compared to hemagglutination inhibition-active antibodies²⁵. Importantly, the correlation of hemagglutinin stalk antibodies with protection from symptomatic influenza was consistent for both children and adults, which may indicate that hemagglutinin stalk antibodies can reduce symptoms at sub-sterilizing levels.

While neuraminidase antibody levels also correlated with protection, the majority of our participants had low baseline neuraminidase antibody levels which limited the power of neuraminidase antibodies as an independent correlate of protection, after adjusting for age and hemagglutination inhibition titers. Furthermore, the results indicated that antibodies against neuraminidase correlated with hemagglutinin antibodies in these individuals, potentially because the antibodies in this largely unvaccinated population were mainly elicited by infections, which would elicit antibodies against both hemagglutinin and neuraminidase. Neuraminidase antibodies correlated more with antibodies against the hemagglutinin stalk (Pearson's $r=0.35$) compared to hemagglutination inhibition active antibodies (Pearson's $r=0.25$; Extended Data Fig. 9). Previous studies have shown that neuraminidase inhibition assays could be a useful correlate of protection from infection^{12,26} but hemagglutinin stalk antibodies can contribute to neuraminidase inhibition measured in the traditional enzyme-linked lectin assay^{17,27–29}. Based on these findings, it is possible that the correlation with protection reported for neuraminidase inhibition is partially conferred by hemagglutinin stalk antibodies. Unfortunately, we did not have sufficient serum specimens to perform neuraminidase inhibition in this study. We also did not perform microneutralization assays, which have been previously shown to correlate with protection from infection, but may not fully capture the specific effects of hemagglutinin stalk antibodies. The protective effect of these non-neutralizing antibodies should be investigated in future studies using assays that measure Fc-mediated functions of antibodies to dissect the mechanisms of antibody-mediated protection. Similarly, cell-mediated immunity could not be assessed in this study and will need to be further investigated. Importantly, these additional immune mechanisms could explain why a subset of adults did not have PCR-confirmed infection, despite low antibody levels.

ELISAs are used as standard assays for a number of other pathogens and are comparatively easy to standardize³⁰. While antibody binding as measured in these assays may not directly translate into functionality, our findings indicate that in a human cohort study setting with individuals who have acquired immunity primarily through virus exposure, results from binding assays could accurately predict protection from infection. We have also previously shown that ELISA antibody levels after vaccination can predict the protection of mice in a human serum transfer experiment⁴. Furthermore, this study shows that these assays can be useful in combination with hemagglutination inhibition assays to assess seroconversion after influenza virus infection.

Hemagglutinin stalk antibodies were measured using a chimeric hemagglutinin antigen, which has an exotic H6 head domain to which humans are generally naïve. However, some rare cross-reactive

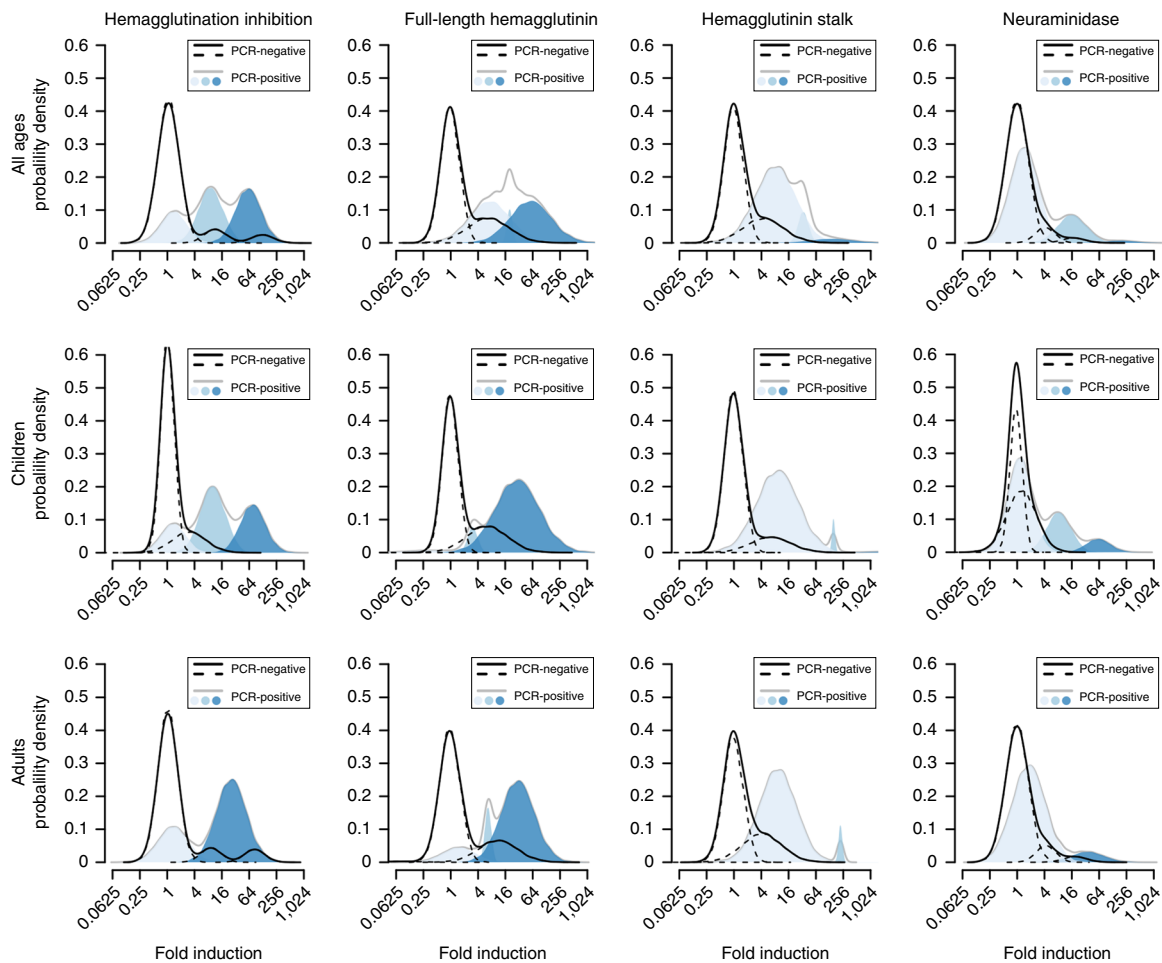


Fig. 4 | Non-responder subpopulation. The black lines indicate the probability density distribution of antibody response among non-infected members. The gray lines encompass the colored subpopulations of antibody response among infected members. The shades of blue indicate the three separate populations calculated by the model. Analyses were performed combined (all ages, $n=300$ individuals) as well as separately for children (0–14 years old, $n=101$ individuals) and adults (15–85 years old, $n=199$ individuals).

head antibodies have been previously described that could recognize conserved epitopes on this antigen^{31,32}. Therefore, it cannot be excluded that part of the measured response is provided by non-hemagglutination inhibition active cross-reactive head antibodies. Since these antibodies have been rarely isolated from humans, the majority of the measured responses are probably hemagglutinin stalk antibodies. Accordingly, antibody levels measured using a chimeric hemagglutinin have been previously shown to correlate well with antibodies measured using headless hemagglutinin probes in ferrets that were vaccinated with multiple heterologous hemagglutinin head domains⁵.

A particular strength of our study was the intensive follow-up that allowed us to capture both symptomatic and asymptomatic individuals, which translated to a high number of observed infections and provided statistical power for our detailed analyses.

The study was performed in Nicaragua where influenza virus vaccination was introduced recently and is not widely used; therefore, the majority of the preexisting antibody response was probably induced by repeated natural infections. This differs from the situation in countries where vaccination rates are high. Similar studies that test highly vaccinated individuals will be required to detect potential differences in protective antibody levels elicited by vaccination versus infection.

In summary, we found that hemagglutinin stalk antibodies are an independent correlate of protection from pandemic H1N1 infection

and disease in a natural transmission setting. Further, antibodies measured by ELISA can be used as a powerful correlate of protection and to assess seroconversion, which will be important for novel universal influenza virus vaccine development^{10,33,34}. Additional resources should be allocated to standardize these assays to enable their use in both research and clinical settings. Further studies are required to examine the role of these antibodies as potential correlates of protection against influenza A (H3N2) and influenza B in natural transmission settings.

Online content

Any methods, additional references, Nature Research reporting summaries, source data, statements of code and data availability and associated accession codes are available at <https://doi.org/10.1038/s41591-019-0463-x>.

Received: 16 October 2018; Accepted: 15 April 2019;
Published online: 3 June 2019

References

1. Nair, H. et al. Global burden of respiratory infections due to seasonal influenza in young children: a systematic review and meta-analysis. *Lancet* **378**, 1917–1930 (2011).
2. Thompson, W. W. et al. Estimates of US influenza-associated deaths made using four different methods. *Influenza Other Respir. Viruses* **3**, 37–49 (2009).

3. Nachbagauer, R. & Krammer, F. Universal influenza virus vaccines and therapeutic antibodies. *Clin. Microbiol. Infect.* **23**, 222–228 (2017).
4. Jacobsen, H. et al. Influenza virus hemagglutinin stalk-specific antibodies in human serum are a surrogate marker for in vivo protection in a serum transfer mouse challenge model. *MBio* **8**, e01463-17 (2017).
5. Nachbagauer, R. et al. A universal influenza virus vaccine candidate confers protection against pandemic H1N1 infection in preclinical ferret studies. *NPJ Vaccines* **2**, 26 (2017).
6. Nachbagauer, R. & Palese, P. Development of next generation hemagglutinin-based broadly protective influenza virus vaccines. *Curr. Opin. Immunol.* **53**, 51–57 (2018).
7. Hobson, D., Curry, R. L., Beare, A. S. & Ward-Gardner, A. The role of serum haemagglutination-inhibiting antibody in protection against challenge infection with influenza A2 and B viruses. *J. Hyg. (Lond.)* **70**, 767–777 (1972).
8. Ohmit, S. E., Petrie, J. G., Cross, R. T., Johnson, E. & Monto, A. S. Influenza hemagglutination-inhibition antibody titer as a correlate of vaccine-induced protection. *J. Infect. Dis.* **204**, 1879–1885 (2011).
9. Potter, C. W. & Oxford, J. S. Determinants of immunity to influenza infection in man. *Br. Med. Bull.* **35**, 69–75 (1979).
10. Erbeling, E. J. et al. A universal influenza vaccine: the strategic plan for the national institute of allergy and infectious diseases. *J. Infect. Dis.* **218**, 347–354 (2018).
11. McElhaney, J. E., Coler, R. N. & Baldwin, S. L. Immunologic correlates of protection and potential role for adjuvants to improve influenza vaccines in older adults. *Expert Rev. Vaccines* **12**, 759–766 (2013).
12. Monto, A. S. et al. Antibody to influenza virus neuraminidase: an independent correlate of protection. *J. Infect. Dis.* **212**, 1191–1199 (2015).
13. Sridhar, S. et al. Cellular immune correlates of protection against symptomatic pandemic influenza. *Nat. Med.* **19**, 1305–1312 (2013).
14. Coudeville, L. et al. Relationship between haemagglutination-inhibiting antibody titres and clinical protection against influenza: development and application of a bayesian random-effects model. *BMC Med. Res. Methodol.* **10**, 18 (2010).
15. Cauchemez, S. et al. Influenza infection rates, measurement errors and the interpretation of paired serology. *PLoS Pathog.* **8**, e1003061 (2012).
16. Chen, Y.-Q. et al. Influenza infection in humans induces broadly cross-reactive and protective neuraminidase-reactive antibodies. *Cell* **173**, 417–429.e10 (2018).
17. Rajendran, M. et al. Analysis of anti-influenza virus neuraminidase antibodies in children, adults, and the elderly by ELISA and enzyme inhibition: evidence for original antigenic sin. *MBio* **8**, e02281-16 (2017).
18. Babu, T. M. et al. Population serologic immunity to human and avian H2N2 viruses in the United States and Hong Kong for pandemic risk assessment. *J. Infect. Dis.* **218**, 1054–1060 (2018).
19. Zost, S. J. et al. Contemporary H3N2 influenza viruses have a glycosylation site that alters binding of antibodies elicited by egg-adapted vaccine strains. *Proc. Natl Acad. Sci. USA* **114**, 12578–12583 (2017).
20. de Vries, R. D. et al. Influenza virus-specific antibody dependent cellular cytotoxicity induced by vaccination or natural infection. *Vaccine* **35**, 238–247 (2017).
21. DiLillo, D. J., Tan, G. S., Palese, P. & Ravetch, J. V. Broadly neutralizing hemagglutinin stalk-specific antibodies require FcγR interactions for protection against influenza virus in vivo. *Nat. Med.* **20**, 143–151 (2014).
22. Park, J. K. et al. Evaluation of preexisting anti-hemagglutinin stalk antibody as a correlate of protection in a healthy volunteer challenge with influenza A/H1N1pdm virus. *MBio* **9**, e02284-17 (2018).
23. Varble, A. et al. Influenza A virus transmission bottlenecks are defined by infection route and recipient host. *Cell Host Microbe* **16**, 691–700 (2014).
24. Ng, S. et al. Estimation of the association between antibody titers and protection against confirmed influenza virus infection in children. *J. Infect. Dis.* **208**, 1320–1324 (2013).
25. He, W. et al. Broadly neutralizing anti-influenza virus antibodies: enhancement of neutralizing potency in polyclonal mixtures and IgA backbones. *J. Virol.* **89**, 3610–3618 (2015).
26. Couch, R. B. et al. Antibody correlates and predictors of immunity to naturally occurring influenza in humans and the importance of antibody to the neuraminidase. *J. Infect. Dis.* **207**, 974–981 (2013).
27. Chen, Y. Q., Lan, L. Y., Huang, M., Henry, C. & Wilson, P. C. Hemagglutinin stalk-reactive antibodies interfere with influenza virus neuraminidase activity by steric hindrance. *J. Virol.* **93**, e01526–18 (2018).
28. Kosik, I. et al. Neuraminidase inhibition contributes to influenza A virus neutralization by anti-hemagglutinin stem antibodies. *J. Exp. Med.* **216**, 304–316 (2019).
29. Wohlbold, T. J. et al. Hemagglutinin stalk- and neuraminidase-specific monoclonal antibodies protect against lethal H10N8 influenza virus infection in mice. *J. Virol.* **90**, 851–861 (2015).
30. Plotkin, S. A. Correlates of protection induced by vaccination. *Clin. Vaccine Immunol.* **17**, 1055–1065 (2010).
31. Ekiert, D. C. et al. Cross-neutralization of influenza A viruses mediated by a single antibody loop. *Nature* **489**, 526–532 (2012).
32. Lee, J. et al. Molecular-level analysis of the serum antibody repertoire in young adults before and after seasonal influenza vaccination. *Nat. Med.* **22**, 1456–1464 (2016).
33. Paules, C. I., Marston, H. D., Eisinger, R. W., Baltimore, D. & Fauci, A. S. The pathway to a universal influenza vaccine. *Immunity* **47**, 599–603 (2017).
34. Paules, C. I., Sullivan, S. G., Subbarao, K. & Fauci, A. S. Chasing seasonal influenza: the need for a universal influenza vaccine. *N. Engl. J. Med.* **378**, 7–9 (2018).

Acknowledgements

The authors thank past and present members of the study team based at the Health Center Sócrates Flores Vivas, the National Virology Laboratory at the Centro Nacional de Diagnóstico y Referencia, and the Sustainable Sciences Institute in Nicaragua for their dedication and high-quality work. We are grateful to the study participants and their families. Lastly, we thank F. Busto Carrillo for assistance in generating the figures. This work was supported by the National Institute for Allergy and Infectious Diseases (award no. R01 AI120997 to A.G. and contract nos. HHSN272201400008C to F.K. and HHSN272201400006C to A.G.). The funders had no role in study design, data collection and analysis, decision to publish, or preparation of the manuscript.

Author contributions

A.G., F.K., S.N. and R.N. designed the study. A.G., G.K., L.G., A.B., S.O., R.L. and N.S. collected the data. M.P., D.S., A.R., R.L., A.F.G. and F.A. generated the laboratory data. S.N., R.N. and A.G. analyzed the data. S.N., R.N., A.G. and F.K. interpreted the data. All authors critically reviewed the paper and approved of the final version of the paper for submission.

Competing interests

The Icahn School of Medicine at Mount Sinai has filed patent applications regarding influenza virus vaccines. The Krammer laboratory receives funding for universal influenza virus vaccine projects from the Department of Defense, PATH, the Bill and Melinda Gates Foundation and GlaxoSmithKline.

Additional information

Extended data is available for this paper at <https://doi.org/10.1038/s41591-019-0463-x>.

Supplementary information is available for this paper at <https://doi.org/10.1038/s41591-019-0463-x>.

Reprints and permissions information is available at www.nature.com/reprints.

Correspondence and requests for materials should be addressed to F.K. or A.G.

Publisher's note: Springer Nature remains neutral with regard to jurisdictional claims in published maps and institutional affiliations.

© The Author(s), under exclusive licence to Springer Nature America, Inc. 2019

Methods

Participants and study procedures. As a part of an observational household transmission study in Nicaragua, participants who lived with an influenza index case in their household were monitored for influenza virus infection. Daily symptoms were assessed, nasal and oropharyngeal swabs were taken every 2–3 d for 10–14 d and blood samples were collected at enrollment as well as 3–5 weeks later to determine infection outcomes and antibody responses. Eligible households included those that: (1) had an index case with a positive QuickVue Influenza A+B rapid test result and with acute respiratory infection symptom onset within the previous 48 h; and (2) had at least one person living with the index case. Details of the study design have been published^{35,36}. Participants were excluded from this analysis if sufficient blood samples were not available. The principles of the Declaration of Helsinki (7th version, 2013) were strictly followed. Ethical approval was obtained from the institutional review boards of the University of Michigan (HUM 00091392) and the Ministry of Health, Nicaragua (CIRE 06/07/10-025). Written informed consent was obtained from all adult participants and proxy written informed consent was obtained for all children. Assent was obtained from children aged 6 and older.

Laboratory methods. Respiratory samples were tested in the Nicaraguan National Virology Laboratory by real-time reverse-transcription PCR (RT-PCR) using standard protocols³⁷. A hemagglutination inhibition assay³⁸ was performed to determine hemagglutination inhibition titers; ELISA was performed to measure binding antibodies to full-length hemagglutinin, hemagglutinin stalk and neuraminidase. ELISAs were performed as described elsewhere⁴. The hemagglutinin full-length constructs corresponded to the vaccine strains during the respective seasons (2013 season, H1 A/California/4/09; 2015 season, H1 A/Michigan/45/15). A chimeric hemagglutinin expressing the head domain from an H6N1 virus (to which humans are naïve) and the stalk domain of pandemic H1N1 influenza virus A/California/4/09 were used to measure hemagglutinin stalk antibodies. The hemagglutinins were expressed as soluble proteins with a trimerization domain to maintain correct protein folding and conformational epitopes as described previously³⁹. The neuraminidase of A/California/4/09 was used to measure neuraminidase-specific antibodies. The neuraminidase was expressed as a soluble antigen with a tetramerization domain to maintain correct folding and enzymatic activity (as measured in neuraminidase star assays)⁴⁰. ELISA values are reported as the AUC. The AUC was chosen because it considers both the end point and the absolute levels of optical density measured at all tested serum dilutions. The AUC calculation (optical density multiplied by serum dilution over the entire curve) was performed in GraphPad Prism 7 (GraphPad Software). All assays were performed by personnel who were blinded to infection status.

Outcomes. The primary outcome was PCR-confirmed influenza; the secondary outcome was symptomatic influenza (PCR-confirmed infection with an episode of fever with cough or sore throat)⁴¹. Antibody response was measured by the ratio between post- and pre-exposure level (preexisting antibody level).

Statistical analyses. Antibody level-specific attack rates were calculated by dividing the number of infected contacts who had a specific baseline antibody titer by the total number of contacts who had the same level of antibody titer. To infer the crude estimates of the 50 and 80% protective levels, we used a 3-parameter logistic regression model (R nplr package v0.1-7) that allowed for a ≤ 1 probability of infection at the lowest detectable level and a ≥ 0 probability of infection at the highest observable level, meaning that incomplete protection can occur at high levels and participants could have preexisting antibodies at levels that were below what was required for complete protection. Two multivariable logistic regression models were used to study the effect of a fourfold antibody level increase on

infection outcome, including (1) a single-assay model where levels of one serology assay and age are predictors and (2) a multi-assay model where levels of multiple assays and age are predictors. The level of pandemic H1N1 influenza virus activity differed between study years and was adjusted for in the analyses. In models 1 and 2, a smoothing spline function was used to model the effect of age on infection risk (R mgcv package v1.8-24). Antibody levels were log-transformed for all analyses; levels below the lowest detectable limit of 1:10 were imputed as 1:5. Individual antibody titer data points were visualized and compared between disease outcome groups using a two-tailed Wilcoxon rank-sum test. A finite mixture model was used to explore underlying non-responder subpopulations based on the observed distribution of the antibody response (R mixtool package v1.0.4). The model estimates the mean and s.d. for each component of the Gaussian mixtures, which were visualized to illustrate the results on antibody response. Receiver operating characteristic curve analysis (R pROC package v1.12.1) was used to estimate the sensitivity and specificity of each assay. Classification and regression tree analyses (R rpart package v4.1-13) were performed to identify the best combination of assays indicated by their positive (PPVs) and negative predictive values (NPVs) in identifying PCR-positive individuals. False discovery rates (FDRs) were calculated in Prism using the two-stage step-up method of Benjamini et al.⁴².

Reporting Summary. Further information on research design is available in the Nature Research Reporting Summary linked to this article.

Data availability

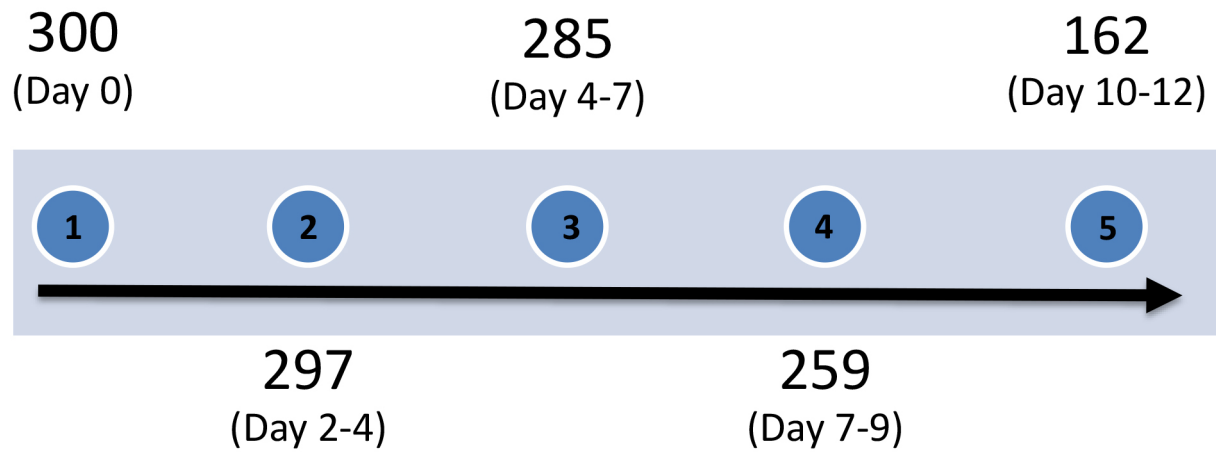
The de-identified data sets used for the study are available on ImmPort (study no. SDY1436). Identifying data required to replicate the study analyses, such as exact age, are available by request as required by the institutional review board-approved protocol for the Nicaragua Household Influenza Transmission Study.

Code availability

Code to understand and assess the conclusions of this research is available via ImmPort (study no. SDY1436).

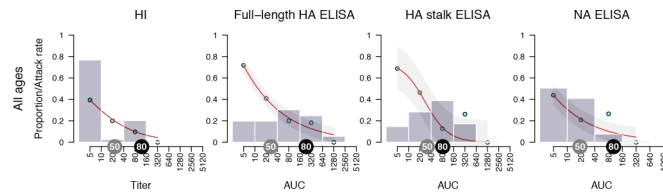
References

- Ng, S. et al. The timeline of influenza virus shedding in children and adults in a household transmission study of influenza in Managua, Nicaragua. *Pediatr. Infect. Dis. J.* **35**, 583–586 (2016).
- Ng, S. et al. Association between haemagglutination inhibiting antibodies and protection against clade 6B viruses in 2013 and 2015. *Vaccine* **35**, 6202–6207 (2017).
- Massingale, S. et al. Emergence of a novel swine-origin influenza A (H1N1) virus in humans. *N. Engl. J. Med.* **360**, 2605–2615 (2009).
- WHO Global Influenza Surveillance Network. *Manual for the Laboratory Diagnosis and Virological Surveillance of Influenza* (World Health Organization, 2011).
- Margine, I., Palese, P. & Krammer, F. Expression of functional recombinant hemagglutinin and neuraminidase proteins from the novel H7N9 influenza virus using the baculovirus expression system. *J. Vis. Exp.* **6**, e51112 (2013).
- Wohlbold, T. J. et al. Vaccination with adjuvanted recombinant neuraminidase induces broad heterologous, but not heterosubtypic, cross-protection against influenza virus infection in mice. *MBio* **6**, e02556 (2015).
- Roush, S. W. et al. (eds) *Manual for the Surveillance of Vaccine-preventable Diseases* (Centers for Disease Control and Prevention, 2008).
- Benjamini, Y., Krieger, A. M. & Yekutieli, D. Adaptive linear step-up procedures that control the false discovery rate. *Biometrika* **93**, 491–507 (2006).

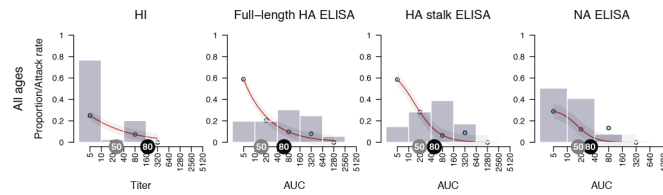


Extended Data Fig. 1 | Participant follow-up timeline. Participant sample collection timeline with the number of samples collected from unique individuals ($n=300$ individuals). Day ranges are represented as quintiles.

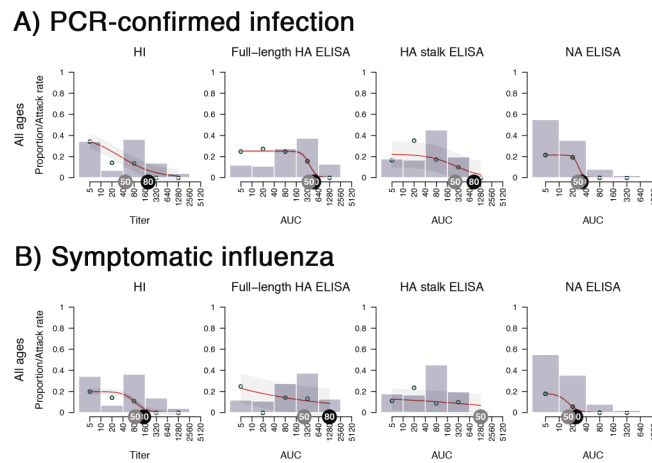
A) PCR-confirmed infection



B) Symptomatic influenza

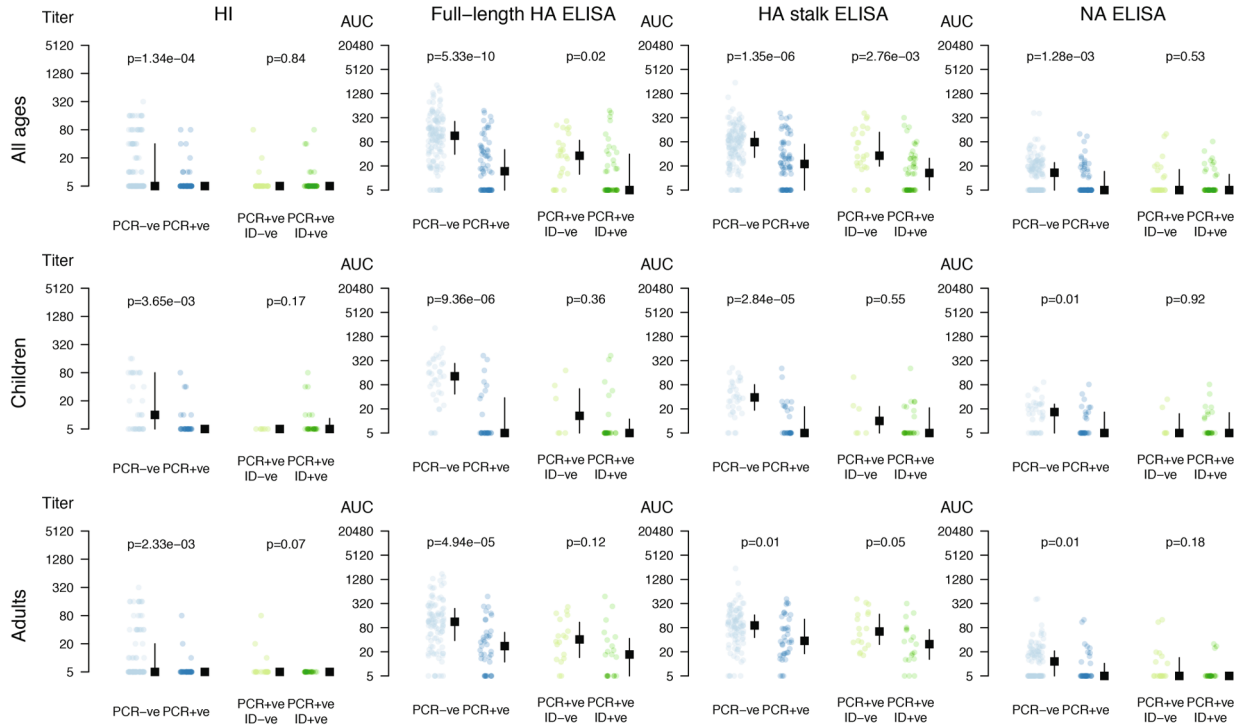


Extended Data Fig. 2 | Preexisting antibodies and corresponding SARs in 2015 ($n = 198$ individuals). **a**, PCR-confirmed infection. **b**, Symptomatic influenza. Note that the geometric mean baseline hemagglutination inhibition titer for this year was 1:10. The gray tags indicate a 50% protection level and the black tags indicate an 80% protection level. The gray bars show the proportion of household contacts having a certain level of preexisting antibody levels. The bars group individuals between the antibody levels covered by the bars on the x axis (for example, the left-most bar includes all individuals with antibody levels <10, followed by 10 but less than 40, etc.). The red lines fit the antibody level-specific SAR based on the observed rates, which are indicated as cyan points. The attack rate was calculated by dividing the number of infected contacts who had a specific baseline antibody level by the total number of contacts who had the same level of antibodies. The shaded area represents the 95% CIs.

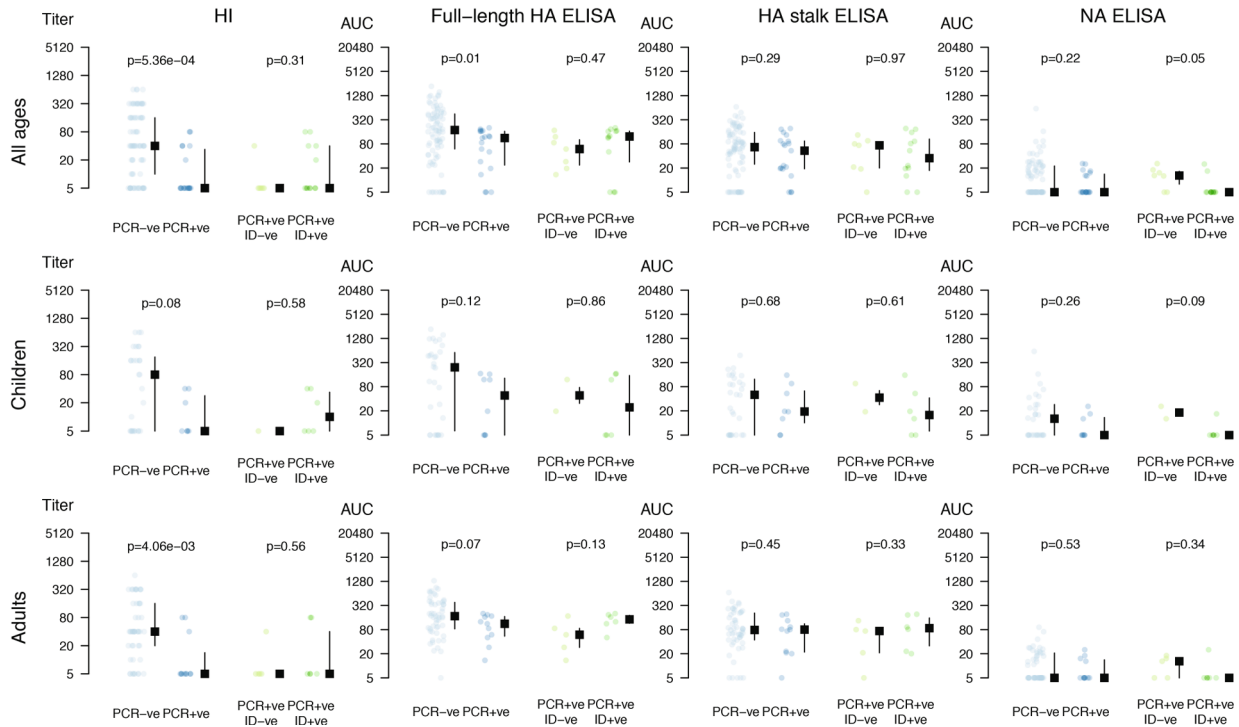


Extended Data Fig. 3 | Preexisting antibodies and corresponding SARs in 2013 ($n = 102$ individuals). **a**, PCR-confirmed infection. **b**, Symptomatic influenza. Note that the geometric mean baseline hemagglutination inhibition titer for this year was 1:34. The gray tags indicate a 50% protection level and the black tags indicate an 80% protection level. The gray bars show the proportion of household contacts having a certain level of preexisting antibody levels. The bars group individuals between the antibody levels covered by the bars on the x axis (for example, the left-most bar includes all individuals with antibody levels <10 , followed by 10 but less than 40, etc.). The red lines show the sigmoid function fitted to the observed antibody level-specific SARs, which are indicated as cyan points. The attack rate was calculated by dividing the number of infected contacts who had a specific baseline antibody level by the total number of contacts who had the same level of antibodies. The shaded area represents the 95% CIs for the predicted antibody level-specific SAR.

A) 2015 A(H1N1)pdm epidemic

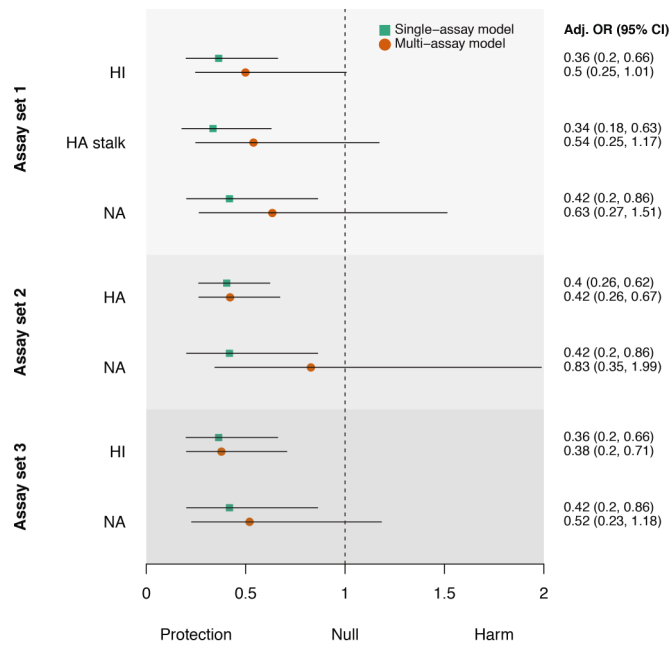


B) 2013 A(H1N1)pdm epidemic

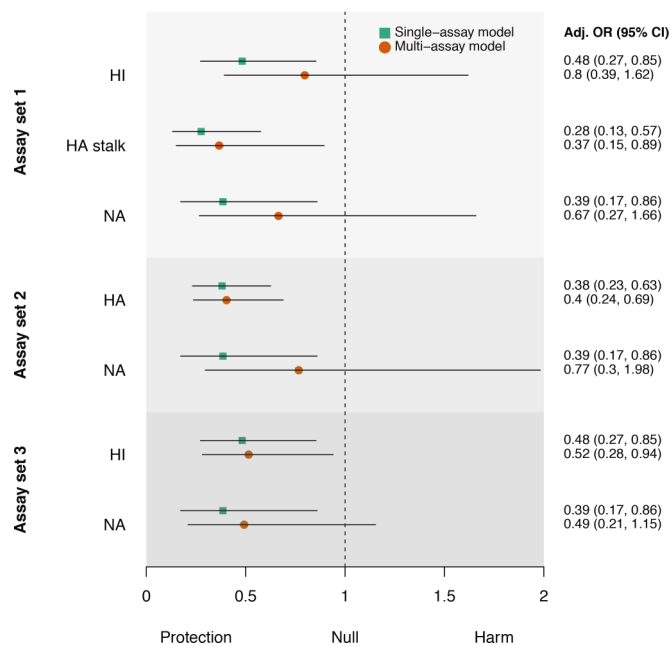


Extended Data Fig. 4 | Influenza outcome-specific distribution of preexisting antibodies. **a**, 2015 influenza A (H1N1) pandemic epidemic. **b**, 2013 influenza A (H1N1) pandemic epidemic. Antibody levels for each individual, and the median and interquartile range, are shown. The y axis indicates the antibody levels. Individuals were separated by PCR-positivity status (blue dots) and by symptomatic influenza (green dots). Individual antibody titer data points were compared between disease outcome groups using a two-tailed Wilcoxon rank-sum test. Analyses were performed combined (all ages; 2013: $n = 102$ individuals; 2015: $n = 198$ individuals) as well as separately for children (0–14 years old; 2013: $n = 38$ individuals; 2015: $n = 64$ individuals) and adults (15–85 years old; 2013: $n = 63$ individuals; 2015: $n = 135$ individuals). See Supplementary Tables 5 and 6 for the FDR analyses. Age groups and outcomes were prespecified before the analyses.

A) PCR-confirmed infection

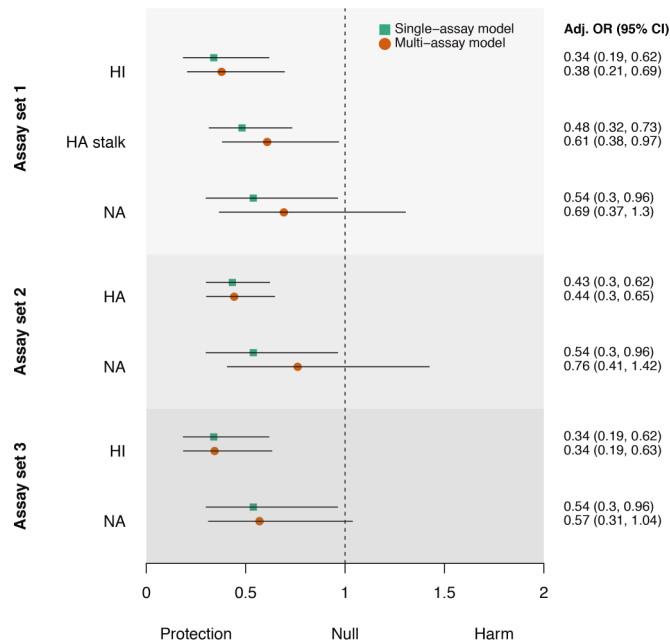


B) Symptomatic influenza

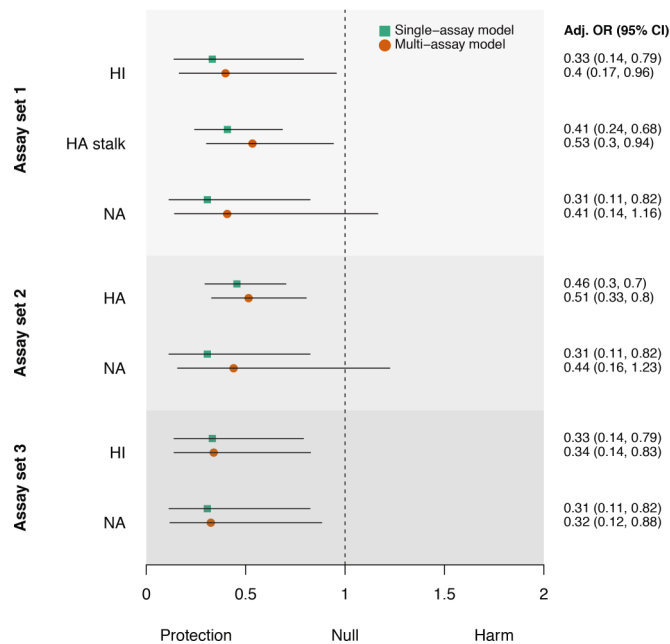


Extended Data Fig. 5 | Protective effects associated with a fourfold increase in antibody level among children. Results are shown for three different sets of assays. **a**, PCR-confirmed infection. **b**, Symptomatic influenza ($n=101$ individuals). Assay set 1 combines hemagglutination inhibition, hemagglutinin stalk and neuraminidase ELISAs. Assay set 2 combines full-length hemagglutinin and neuraminidase ELISAs. Assay set 3 combines hemagglutination inhibition and neuraminidase ELISAs. Adjusted ORs for the single-assay model are shown as green squares and the multi-assay model as orange circles. The black lines denote the 95% CIs.

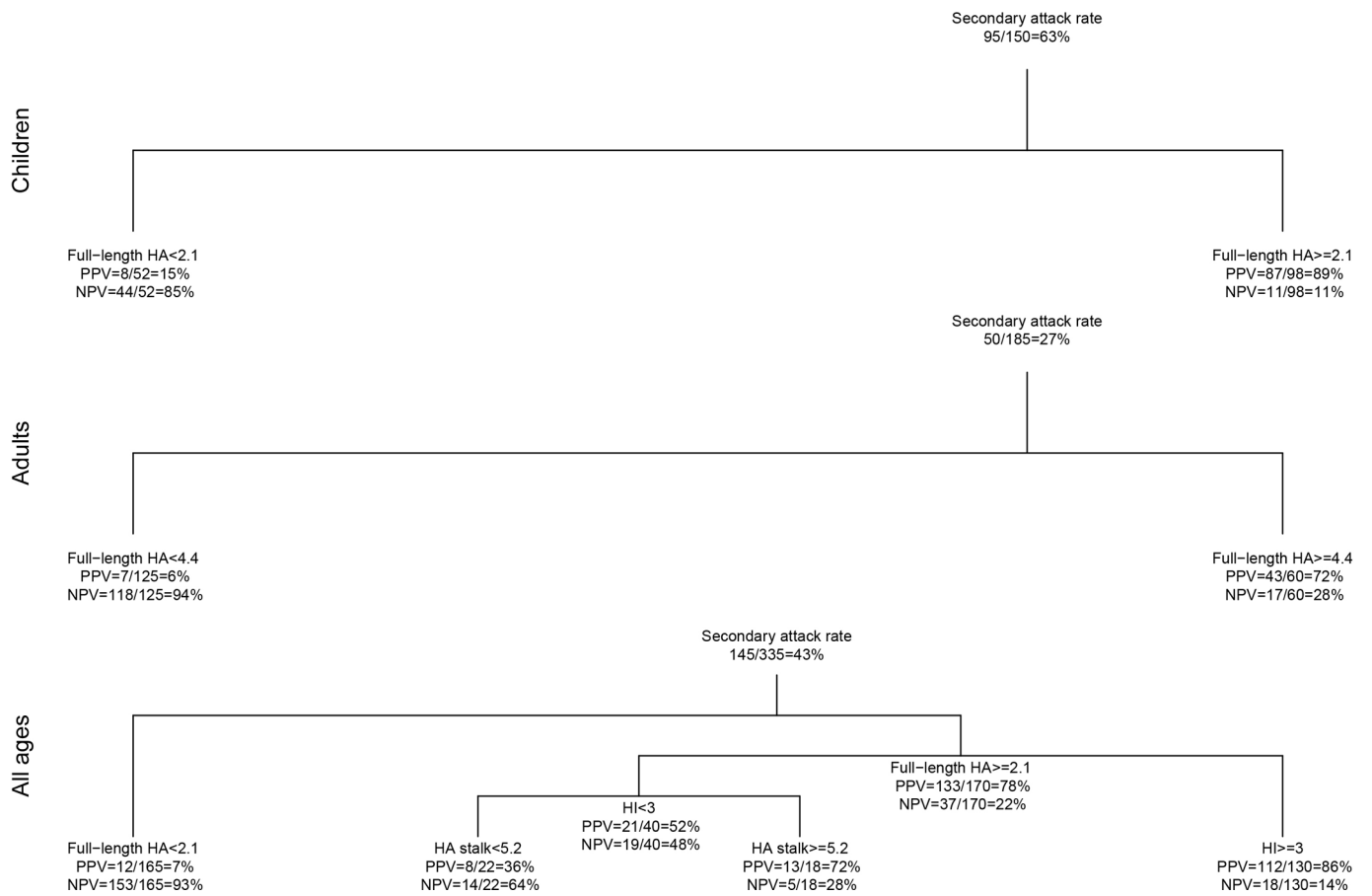
A) PCR-confirmed infection



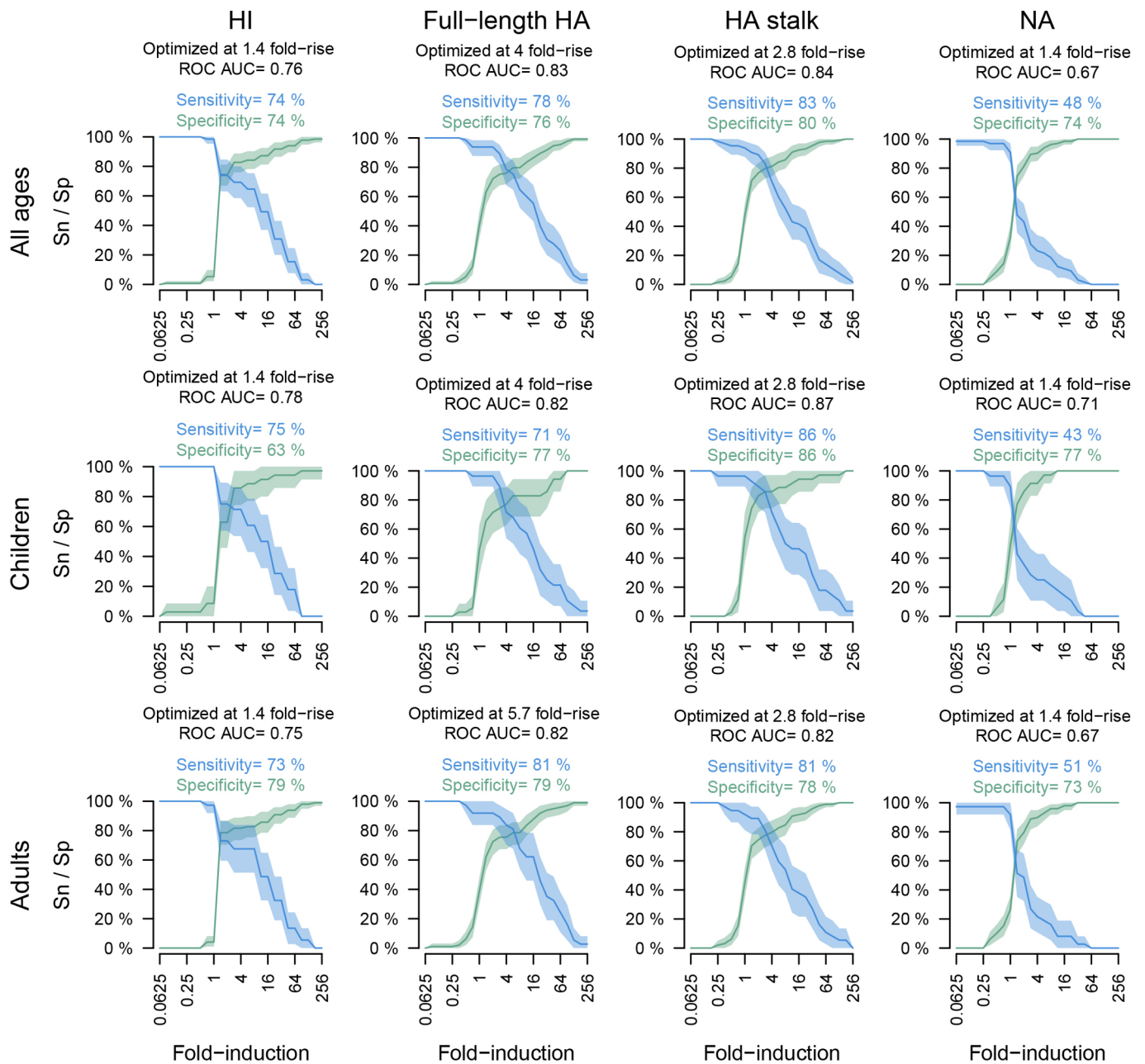
B) Symptomatic influenza



Extended Data Fig. 6 | Protective effects associated with a fourfold increase in antibody level among adults. Results are shown for three different sets of assays. **a**, PCR-confirmed infection. **b**, Symptomatic influenza ($n=199$ individuals). Assay set 1 combines hemagglutination inhibition, hemagglutinin stalk and neuraminidase ELISAs. Assay set 2 combines full-length hemagglutinin and neuraminidase ELISAs. Assay set 3 combines hemagglutination inhibition and neuraminidase ELISAs. Adjusted ORs for the single-assay model are shown as green squares and the multi-assay model as orange circles. The black lines denote the 95% CIs.

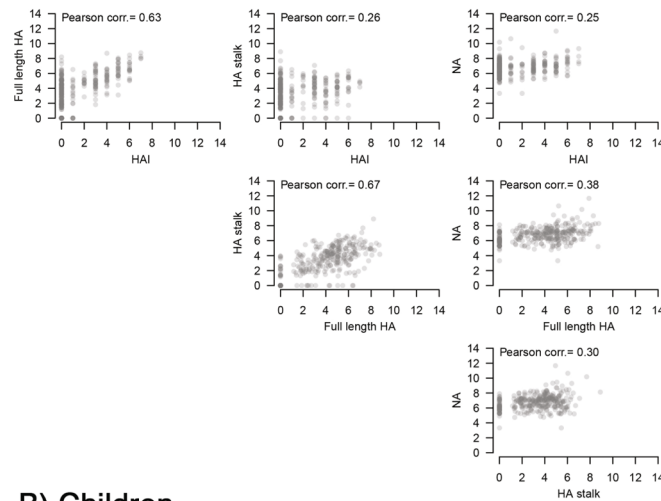


Extended Data Fig. 7 | PPVs and NPVs of the best serology testing strategy identified by decision tree analyses. True positive cases were individuals who had PCR-confirmed influenza virus infection. True negative cases were individuals who had neither a positive PCR nor a fourfold rise in antibody serology tests. The model also suggested optimal cutoff points to use when defining seroconversion.

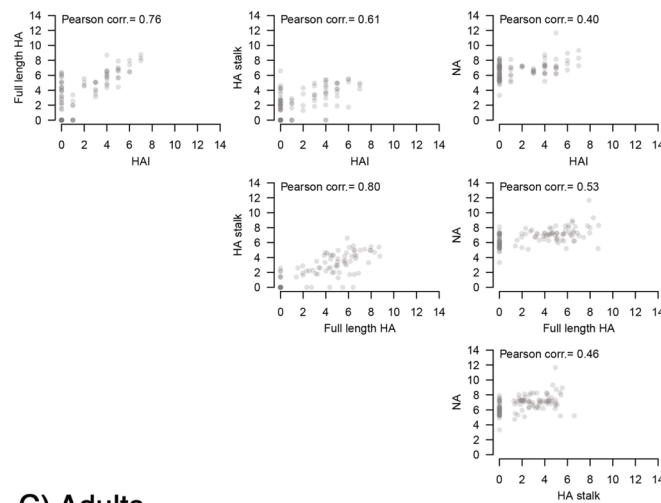


Extended Data Fig. 8 | Sensitivity and specificity of hemagglutination inhibition and ELISA in detecting PCR-confirmed infections. Curves are plotted as solid lines for sensitivity (Sn) in blue and specificity (Sp) in green. The shaded areas indicate the 95% CIs. The x axes show the fold induction for the respective assay. Analyses were performed combined (all ages, $n=300$) as well as separately for children (0-14 years old, $n=101$) and adults (15-85 years old, $n=199$).

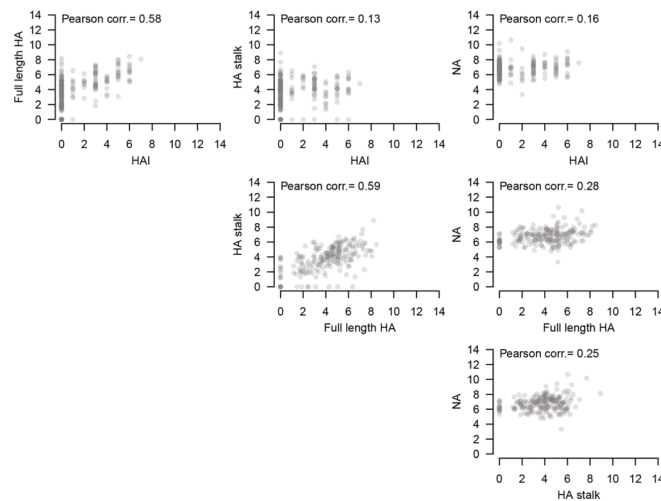
A) Combined titers



B) Children



C) Adults



Extended Data Fig. 9 | Antibody titer correlations. **a-c**, Correlation analyses for antibody titers were performed combined (all ages, $n=300$ individuals) (**a**) as well as separately for children (0–14 years old, $n=101$ individuals) (**b**) and adults (15–85 years old, $n=199$ individuals) (**c**). Pearson's r is plotted in each figure.

Reporting Summary

Nature Research wishes to improve the reproducibility of the work that we publish. This form provides structure for consistency and transparency in reporting. For further information on Nature Research policies, see [Authors & Referees](#) and the [Editorial Policy Checklist](#).

Statistical parameters

When statistical analyses are reported, confirm that the following items are present in the relevant location (e.g. figure legend, table legend, main text, or Methods section).

n/a Confirmed

- The exact sample size (n) for each experimental group/condition, given as a discrete number and unit of measurement
- An indication of whether measurements were taken from distinct samples or whether the same sample was measured repeatedly
- The statistical test(s) used AND whether they are one- or two-sided
Only common tests should be described solely by name; describe more complex techniques in the Methods section.
- A description of all covariates tested
- A description of any assumptions or corrections, such as tests of normality and adjustment for multiple comparisons
- A full description of the statistics including central tendency (e.g. means) or other basic estimates (e.g. regression coefficient) AND variation (e.g. standard deviation) or associated estimates of uncertainty (e.g. confidence intervals)
- For null hypothesis testing, the test statistic (e.g. F , t , r) with confidence intervals, effect sizes, degrees of freedom and P value noted
Give P values as exact values whenever suitable.
- For Bayesian analysis, information on the choice of priors and Markov chain Monte Carlo settings
- For hierarchical and complex designs, identification of the appropriate level for tests and full reporting of outcomes
- Estimates of effect sizes (e.g. Cohen's d , Pearson's r), indicating how they were calculated
- Clearly defined error bars
State explicitly what error bars represent (e.g. SD, SE, CI)

Our web collection on [statistics for biologists](#) may be useful.

Software and code

Policy information about [availability of computer code](#)

Data collection

All clinical data was recorded using OpenClinica. Laboratory data was collected in Microsoft Access.

Data analysis

To infer the crude estimates of the 50% and 80% protective levels, we used a 3-parameter logistic regression model (nplr R package v0.1-7). In models 1 and 2, a smoothing spline function was used to model the effect of age on infection risk (mgcv R package v1.8-24). A mixture model was used to explore underlying non-responder sub-populations based on the observed distribution of the antibody response (mixtool R package v1.0.4). Receiver Operating Characteristic Curve (ROC) analysis (pROC R package v1.12.1) was used to estimate the sensitivity and specificity of each assay. Classification and Regression Trees analysis (rpart R package v4.1-13) were performed to identify the best combination of assays indicated by their positive and negative predictive values in identifying PCR positive individuals. False discovery rates (FDR) were calculated in GraphPad Prism (v7.04) using the two-stage step-up method of Benjamini, Krieger and Yekutieli.

For manuscripts utilizing custom algorithms or software that are central to the research but not yet described in published literature, software must be made available to editors/reviewers upon request. We strongly encourage code deposition in a community repository (e.g. GitHub). See the Nature Research [guidelines for submitting code & software](#) for further information.

Data

Policy information about [availability of data](#)

All manuscripts must include a [data availability statement](#). This statement should provide the following information, where applicable:

- Accession codes, unique identifiers, or web links for publicly available datasets
- A list of figures that have associated raw data
- A description of any restrictions on data availability

All data to understand and assess the conclusions of this research are available in the main text, supplementary materials, and via ImmPort. Data are available by request, as is required by the institutional review board–approved protocol for the Household Influenza Transmission Study.

Field-specific reporting

Please select the best fit for your research. If you are not sure, read the appropriate sections before making your selection.

Life sciences Behavioural & social sciences Ecological, evolutionary & environmental sciences

For a reference copy of the document with all sections, see nature.com/authors/policies/ReportingSummary-flat.pdf

Life sciences study design

All studies must disclose on these points even when the disclosure is negative.

Sample size	All persons in the study with sufficient sample volume and type during the included years were included in the study. Based on infection probabilities, an r-squared of 0.5-0.7, an alpha of 0.05 a sample size of 46-134 is required for 80% power. Thus, the sample size of 300 used in the analyses gives >80% power.
Data exclusions	Participants were excluded from this analysis if sufficient blood samples were not available.
Replication	Replication was not performed.
Randomization	Randomization was not performed. Samples were allocated based on whether or not the individual tested positive by RT-PCR for influenza. Age was included in all analyses as a covariate.
Blinding	All assays were performed by personnel blinded to infection status.

Reporting for specific materials, systems and methods

Materials & experimental systems

n/a	Involved in the study
<input checked="" type="checkbox"/>	<input type="checkbox"/> Unique biological materials
<input checked="" type="checkbox"/>	<input type="checkbox"/> Antibodies
<input checked="" type="checkbox"/>	<input type="checkbox"/> Eukaryotic cell lines
<input checked="" type="checkbox"/>	<input type="checkbox"/> Palaeontology
<input checked="" type="checkbox"/>	<input type="checkbox"/> Animals and other organisms
<input type="checkbox"/>	<input checked="" type="checkbox"/> Human research participants

Methods

n/a	Involved in the study
<input checked="" type="checkbox"/>	<input type="checkbox"/> ChIP-seq
<input checked="" type="checkbox"/>	<input type="checkbox"/> Flow cytometry
<input checked="" type="checkbox"/>	<input type="checkbox"/> MRI-based neuroimaging

Human research participants

Policy information about [studies involving human research participants](#)

Population characteristics	During the 2013 and 2015 influenza A(H1N1)pdm epidemics, 300 household members who lived with one of 88 index cases were followed for 3-5 weeks to test for infection and seroconversion. If the 300 participants, 101 were children between the ages of 0-14 years and 199 were aged 15 or more years. There were 101 females and 199 males in the study.
Recruitment	Eligible households included those that 1) had an index case that had a positive QuickVue Influenza A+B rapid test result and with acute respiratory infection (ARI) symptom onset within the previous 48 hours; and, 2) had at least one person living with the index case. Given that only 3% of houses (5/165) approached declined participation and only 1% (9/786) of potential

participants in enrolled houses declined participation, we think that it is very unlikely that it is very unlikely that self-selection bias has biased the results of the study.